Search for WZ Production in the $\mu\nu ee$ Decay Channel

DØ Note 3529

October, 1998

Patrick Gartung

University of California, Riverside, CA 92521

1 Introduction

WZ production in the $l\nu ll$ channel is relatively background free and a search for this process in the Run 1 data can be used to set limits on the WZ production cross section and on anomalous WWZ couplings. An analysis based on the $e\nu ee$ decay channel was presented in an earlier DØ note [1]. In this note we present an analysis based on the $\mu\nu ee$ decay channel. This analysis is a relatively simple extension of the previous $e\nu ee$ analysis because the same two-EM object trigger can be used and the event selection requirements are similar, except for the requirement of a high-p_T isolated muon in place of the third electron. The data used in this analysis is from the Run 1b and Run 1c data samples.

2 Particle Identification

2.1 Electron Identification

Electrons are corrected to the vertex found by cluster-track projection as detailed in [1] and [2]. The following cuts are used for tight and loose quality electrons:

- CC electrons: $|\eta_{det}| < 1.0$ and $|\Delta\phi(\text{cluster,crack})| > 0.01$ radians
- EC electrons: $1.5 < |\eta_{det}| < 2.5$
- Tight Electron
  - Isolation $I < 0.10$
  - H-matrix $\chi^2 < 100, 200$ (CC,EC)
  - A matching track with significance $\sigma_{track} < 5, 10$ (CDC,FDC)
- Loose Electron
  - Isolation $I < 0.10$
  - H-matrix $\chi^2 < 100, 200$ (CC,EC)
  - Number of hits on drift chamber wires $>$ 20, 36 (CDC,FDC) or a matching track with significance $\sigma_{track} < 5, 10$ (CDC,FDC)

2.2 Muon Identification

The following quality cuts were used to select the muon:

- $|\eta| < 1.0$
- IFW4$\leq$1
- HFRAC$\geq$0.70
- $|xy$ impact parameter$| \leq 25$ cm
- Floating time offset ($|t_0^{float}|$) ≤ 200 ns
- $\int \vec{B} \cdot \vec{dl} \geq 0.6$ GeV
- $\Delta R(\mu, jet) \geq 0.5$ for $E_T^{jet} > 10$ GeV

The first cut allows only muons in the CF region, eliminating punch-through and combinatoric backgrounds. The second cut is on the quality of the muon track fit. The third cut is used to ensure that the muon deposits energy in its passage through the calorimeter, thus rejecting fake muon tracks due to noise hits. The fourth and fifth cuts are used to reject cosmic muons, which do not necessarily pass near the beam line and which arrive out of time with the beam crossing.

Since these identification cuts are identical to those used in the $WW \rightarrow$ dileptons Run 1b analysis [3, 4], we use the efficiencies calculated in that analysis, which are detailed in reference [3]. The efficiencies for each cut were determined from a combination of Monte Carlo and data. The IFW4 and $\int \vec{B} \cdot \vec{dl}$ cuts were determined from MUSMEARED GEANT events, and the efficiencies of the remaining cuts were determined from data. The efficiency of each cut, except the IFW4 and $\int \vec{B} \cdot \vec{dl}$ cut, was determined using $Z \to \mu\mu$ events. The efficiencies were determined for muons in the pre-shutdown and post-shutdown periods and were averaged according to the integrated luminosity in each period. The overall efficiency for muons with $p_T > 15$ GeV was determined to be 0.701 ± 0.031.

3 Event Selection and Detection Efficiency

A search for candidate events was performed using the $Z \to ee$ data sample which has an integrated luminosity of 92.3 ± 4.9 pb^{-1} when events within the MRBS_LOSS and MICRO_BLANK gate are rejected.

The following cuts were used:

- Events within the MRBS_LOSS and MICRO_BLANK gate are rejected;
- Events must pass the EM2_EIS2_HI trigger;
- Events must have one tight electron with $E_T > 25$, one loose electron with $E_T > 25$ GeV and one muon with $p_T > 15$ GeV ;
- Events must have muon-corrected and calorimeter missing transverse energy $\not{E}_T > 15$ GeV.

The calorimeter missing energy cut ensures that the missing energy is real and not just an artifact of a mismeasured muon. No events are observed with this minimal set of cuts.

Modeling of standard-model events and events with anomalous couplings was performed using the event generator of Hagiwara, Woodside and Zeppenfeld [7] followed by a detailed fast Monte Carlo simulation of the DØ detector [5]. The modeling of electrons in the fast simulation was described in [1]. The modeling of muons is described here. The muon momentum is smeared according to the resolution function

$$\left(\frac{\sigma_{1/p}}{(1/p)}\right)^2 = (a(p-p_0)/p)^2 + (bp)^2$$

where a, b, and p_0 are determined from data [6]. The efficiency for muons is modeled using an $\eta - \phi$ efficiency map which accounts for the numerous cracks and holes in the muon system. The efficiency for detecting SM events was determined to be (11.5 $\pm$ 0.15)%. The SM expectation for the $\mu\nu ee$ channel is 0.099 $\pm$ 0.001 (stat) $\pm$ 0.009 (syst) events, based on the leading order cross section of 2.6 pb [7], which includes a k-factor to account for higher order QCD corrections.

4 Backgrounds

As in the $e\nu ee$ channel the backgrounds for this channel come from processes in which a jet fakes the signature of an isolated lepton. The backgrounds include $ee + jet$ events where the jet produces an isolated muon and $e\mu + jet$ events where the jet fakes an electron. In both cases missing energy can result from the mismeasurement of the jet or muon, and therefore a data-based technique must be used to estimate the backgrounds.

Before proceeding it is necessary to calculate the probability of a jet producing an isolated muon. This probability was calculated by counting the number of multijet events with an isolated muon. For a muon with $p_T > 15$ GeV this probability was found to be 1.5×10^{-5} [3]. In addition, the probability of a jet faking a muon from a heavy quark (b/c) jet was found by requiring a muon (isolated or non-isolated) in the opposite hemisphere from the isolated muon. This gave a heavy quark enhanced fake rate of 2.5×10^{-4}. A systematic uncertainty of 10% percent is assigned to both probabilities because of the small number of events with an isolated muon.

To calculate the $ee + jet$ event background, events with two electrons and a central jet were selected from the $Z \to ee$ sample. Each event was required to pass all cuts except that the jet was only required to pass the muon fiducial and kinematic cuts. The number of events (88) is then multiplied by the probability of the jet producing an isolated muon. The number of events expected from this background is ≤ 0.002. A small fraction of the $ee + jet$ events contain real heavy quark (b/c) jets. Assuming that all of the jets in the fake sample are heavy quark jets and using the heavy quark enhanced fake rate, we obtain an upper limit of $N_{\rm bkg} = 0.022$ for this background. However, to set a conservative limit, we take the smaller estimate and neglect this background.

The second background ($e\mu + jet$ events) was calculated from the electroweak group's Run Ib $W \to e\nu$ data sample. Events in this sample required one EM object above 10 GeV and $\not\!\!E_T > 15$ GeV. A background data sample was selected by requiring events with an isolated muon, one or more jets and a tight or loose electron. All event selection cuts were applied with the exception of the trigger, which was replaced by the EM1_EIS_TRKCC trigger. This trigger required one EM object and missing energy at level 2. A total of 60 events were selected, The number of fake events is then found by multiplying by the E_T-dependent probability for a jet to fake an electron, accounting correctly for events which contain more than one jet:

$$N_{\text{bkg}} = w_{\text{trig}} \sum_{j=1}^{N_{\text{evt}}} \left(\sum_{i=1}^{N_{\text{jet}}} P_i(E_T) \right)$$

where N_{bkg} is the estimated number of background events, N_{evt} is the number of events in the background data sample, N_{jet} is the number of jets in the event, $P_i(E_T)$ is the E_T-dependent probability for jet i to fake an electron, and w_{trig} is a factor to account for triggers (see below). Using this method, each jet in the event is considered. The E_T-dependent probability of the jet faking a tight or loose electron was taken from the the $e\nu ee$ channel analysis [1]. The factor w_{trig} is the total integrated luminosity of Runs 1b and 1c divided by the integrated luminosity of Run 1b. This factor was necessary due to the lack of the EM1_EIS_TRKCC trigger in Run 1c. Therefore, only Run 1b data was used to estimate the background and a simple scaling of the background in Run 1c was assumed. The total number of background events expected from $e\mu + jet$ events is $0.118 \pm 0.018(\text{stat}) \pm 0.035(\text{sys})$. The systematic error is due to the 30% error on the probability that a jet fakes an electron [1].

The total number of background events from both sources of background is $0.118 \pm 0.018(\text{stat}) \pm 0.035(\text{syst})$.

5 Limit Setting

An upper limit on the cross section can be set using the TOP_LIMIT routine. The details of this routine can be found in Reference [8].

Because of the small number of observed events Poisson statistics are used in setting limits on the coupling parameters. The Poisson probability of observing n events for a given mean value μ is

$$\frac{e^{-\mu}\mu^n}{n!}$$

The predicted mean number of events is given by

$$\mu = \mu_s + \mu_b. \tag{1}$$

$\mu_s = \mathcal{L}\,\epsilon\,\sigma$ is the expected number of signal events found by multiplying together the integrated luminosity $\mathcal{L}$, the detection efficeincy ϵ and cross section σ. μ_b is the expected number of background events.

However, μ_s and μ_b are not known precisely. Construction of the appropriate probability is facilitated by the introduction of a set of normalization parameters $\{x_i\}$. The probability density describing each of the $\{x_i\}$ is assumed to be described by a normalized Gaussian $g_i(x_i, \sigma_i)$ centered at unity:

$$g_i(x_i, \sigma_i) = \frac{\exp[(x_i - 1)^2/2\sigma_i^2]}{\int_0^\infty \exp[(x_i - 1)^2/2\sigma_i^2]dx_i} \tag{2}$$

where the unphysical region $x_i < 0$ has been excluded. The mean number of expected events is

$$\mu_x = x_s\,\mathcal{L}\epsilon\sigma + x_b\,\mu_b \tag{3}$$

where x_s represents the signal prediction normalization and x_b is the background normalization. (By construction, the central value of all $\{x_i\}$ is one.) Thus, the probability for the ensemble of candidate events is given by

$$P = \int g_s\,g_b\,\frac{e^{-\mu_x}\mu_x^N}{N!}\,dx_s\,dx_b \tag{4}$$

where N is the number of candidates, and μ_x is given by Equation 3.

When combining results from more than one channel, it is important to account for correlations in the uncertainties between the channels. For the case of the $e\nu ee$ and $\mu\nu ee$ channels, there are both common and channel-specific normalization uncertainties for both background and signal predictions. The mean number of $e\nu ee$ events becomes

$$\mu_{eee} = x_{s,c}\, x_{s,eee}\, \mathcal{L}\epsilon\sigma_{eee} + x_{b,c}\, x_{b,eee}\, \mu_{b,eee} \tag{5}$$

where $x_{s,c}$ represents the common signal prediction normalization, $x_{s,eee}$ is the channel-specific signal prediction normalization, $x_{b,c}$ is the common background normalization, and $x_{b,eee}$ is the channel-specific background normalization. The mean number of $\mu\nu ee$ events becomes

$$\mu_{\mu ee} = x_{s,c}\, x_{s,\mu ee}\, \mathcal{L}\epsilon\sigma_{\mu ee} + x_{b,c}\, x_{b,\mu ee}\, \mu_{b,\mu ee} \tag{6}$$

where the notation is similar to that used in Equation 5. The probability function for both channels becomes

$$\begin{aligned} P \;=\; & \int g_{s,c}\, g_{b,c}\, g_{s,eee}\, g_{b,eee}\, g_{s,\mu ee}\, g_{b,\mu ee} \\ & \times \left(\frac{e^{-\mu_{eee}} \mu_{eee}^{N}}{N!} \right) \left(\frac{e^{-\mu_{\mu ee}} \mu_{\mu ee}^{M}}{M!} \right) \\ & \times dx_{s,c}\, dx_{b,c}\, dx_{s,eee}\, dx_{b,eee}\, dx_{s,\mu ee}\, dx_{b,\mu ee} \end{aligned} \tag{7}$$

where N is the number of observed $e\nu ee$ events, M is the number of observed $\mu\nu ee$ events, and μ_{eee} and $\mu_{\mu ee}$ are given by Equations 5 and 6 respectively.

The sources of common predicted signal normalization uncertainty are the di-electron selection efficiency error (0.98%), luminosity error (5.4%), theoretical cross section error (6.2%) and trigger efficiency error (2%). Added in quadrature they give $\sigma_{c,s} = 8.5\%$.

The individual signal uncertainties come from identifying the third lepton, 4.4% for the muon and 0.7% for the electron.

Both the $e\nu ee$ and $\mu\nu ee$ background estimates are based on the jet misidentification probabilities for electrons, which has a 30% normalization uncertainty. Therefore $\sigma_{c,b} = 0.30$.

The individual background uncertainties come from the statistical error on the background. This uncertainty was 18% for the $e\nu ee$ channel and 15% for the $\mu\nu ee$ channel.

$\sigma_{s,c}$	$=$	0.085
$\sigma_{b,c}$	$=$	0.30
$\sigma_{s,eee}$	$=$	0.007
$\sigma_{b,eee}$	$=$	0.18
$\sigma_{s,\mu ee}$	$=$	0.044
$\sigma_{b,\mu ee}$	$=$	0.15

Table 1: Summary of uncertainties for combined probability function.

Equations 2–7 provide a means of calculating the probability of observing N events for given values of the WWZ coupling parameters. In order to sufficiently determine $P(N;\mu(\Delta g_1^Z, \lambda_Z))$, knowledge of μ_s is required for many values of Δg_1^Z and λ_Z. The computational burden is reduced by constructing a 3×3 grid of μ_s values which are obtained from the fast detector simulation for $\Delta g_1^Z = \{0, \pm x_0\}$ and $\lambda_Z = \{0, \pm y_0\}$, where x_0 and y_0

are chosen to be outside the limits being set. Biquadratic interpolation [2] is then used to evaluate μ_s for given values of Δg_1^Z and λ_Z. (The accuracy of this technique was verified by comparing interpolated values with those obtained directly from the simulation at various points in the Δg_1^Z-λ_Z plane.)

Once the probability at each point in the $(\Delta g_1^Z, \lambda_Z)$–plane is known limits can be set. The limits are found by taking the log of the probability and finding the coutour where

$$L = L_{max} - \delta.$$

To set a 95% CL limit in one dimension, the contour is evaluated at $\delta = 1.92$. To set a 95% CL limit in two dimensions, the contour is evaluated at $\delta = 3.00$.

6 Results

The results of this analysis are summarized in Table 2, together with the results from the $e\nu ee$ channel analysis [1].

	$e\nu ee$	$\mu\nu ee$
$N_{\rm data}$	1	0
$N_{\rm bkg}$	$0.38 \pm 0.07 \pm 0.12$	$0.118 \pm 0.018 \pm 0.035$
$N_{\rm SM}$	$0.146 \pm 0.002 \pm 0.011$	$0.099 \pm 0.001 \pm 0.009$

Table 2: Results of the $\mu\nu ee$ analysis and the $e\nu ee$ analysis.

The 95% CL upper limit on the WZ production cross section from the $\mu\nu ee$ channel was found to be 81.2 pb. This is to be compared with a Standard Model cross section for WZ

production of 2.6 pb. Combining with the the previous analysis of the $e\nu ee$ channel (which yielded $\sigma \leq 74.0$ pb), we obtain a combined 95% CL upper limit of 44.3 pb.

The 1-dimensional 95% CL limits on anomalous couplings from the $\mu\nu ee$ channel alone are

$$|\Delta g_1^Z| < 2.51 \text{ for } \lambda_Z = 0$$

$$|\lambda_Z| < 2.07 \text{ for } \Delta g_1^Z = 0.$$

The 1-dimensional 95% CL limits on anomalous couplings from the $e\nu ee$ channel alone are

$$|\Delta g_1^Z| < 2.40 \text{ for } \lambda_Z = 0$$

$$|\lambda_Z| < 1.98 \text{ for } \Delta g_1^Z = 0.$$

The 1-dimensional 95% CL limits using both channels are

$$|\Delta g_1^Z| < 1.63 \text{ for } \lambda_Z = 0$$

$$|\lambda_Z| < 1.42 \text{ for } \Delta g_1^Z = 0.$$

Figure 1 shows the 2-dimensional 95% CL contour limits for the $e\nu ee$ and $\mu\nu ee$ data combined.

References

[1] P. Gartung, "Search for WZ Production in the Tri-lepton + Missing Energy Decay Channel.", DØ Note 3397, May 1998.

[2] S. Glenn, *A Search for Self Interactions of Neutral Electroweak Gauge Bosons.* Ph.D. thesis, University of California at Davis, Davis, California, 1996 (Unpublished).

[3] P. Bloom. *Investigation of the Trilinear Vector Boson Couplings Through W Boson Pair Production in the Dilepton Decay Channels* Ph.D. thesis, University of California at Davis, Davis, California, 1998 (Unpublished).

[4] B. Abbot *et. al.* (DØ Collaboration), to be published in *Phys. Rev.* **D**, Rapid Communications (1998), FERMILAB PUB 98-076-E, hep-ex/9803004

[5] S. Glenn, "A Parametric Detector Simulation for Dibosons." DØ Note 2846 , 1996.

[6] D. Wood, *et. al.* , DØNote 2140.

[7] K. Hagiwara, J. Woodside, and D. Zeppenfeld, *Phys. Rev.* **D41**, 2113 (1990).

[8] R. Partridge "Top Limit Calculation." DØ Note 1806, 1993.

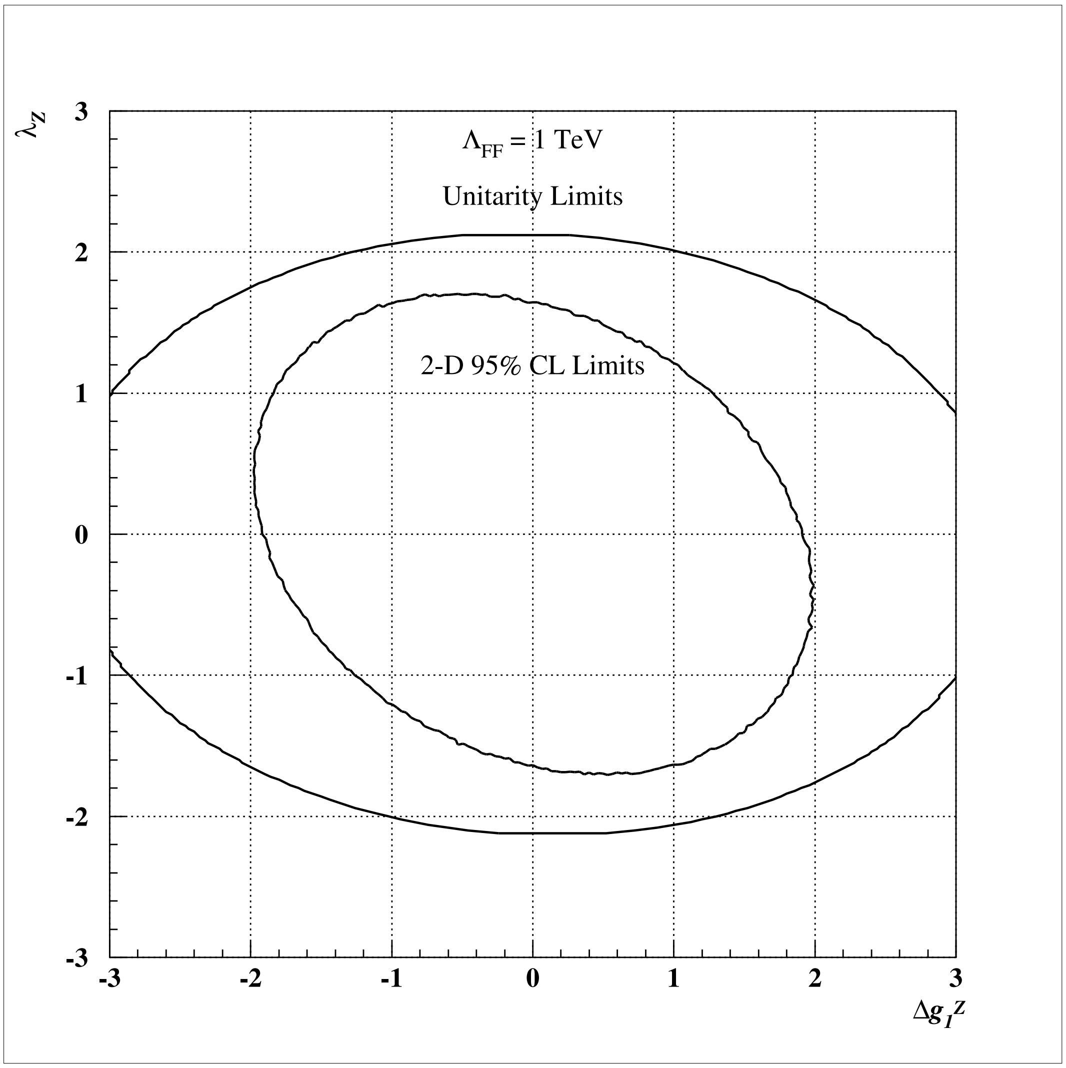

Figure 1: Correlated limits on Δg_1^Z and λ_Z for $\Lambda_{FF} = 1$ TeV obtained from fit to the cross section using the run 1b + 1c data for the $\mu\nu ee$ and $e\nu ee$ channel combined. The inner curve is the 2-dimensional 95% CL contour and the outer curve is the unitarity bound.